UV-light Photocatalytic Activity of Biocompatible Nanoparticles Provide Multiple Effects

S. Harinee, K. Muthukumar, A. Abirami, K. Amrutha, K. Dhivyaprasath, M. Ashok*

Department of Physics, National Institute of Technology (NIT), Tiruchirappalli 620 015, Tamil Nadu, India

*Corresponding author: E-mail: ashokm@nitt.edu

DOI: 10.5185/amp.2019.0006
www.vbripress.com/amp

Abstract

Biocompatible silver (Ag) nanoparticles (NPs) were demonstrated using silver nitrate ($AgNO_3$) and egg white extracted (EWE). Egg white mediated AgNPs were characterized and study its antimicrobial activity against human pathogenic bacteria (HPB), and under UV-light irradiation, photocatalytic degradation of methylene blue (MB) has been studied. Results showed that EWE-AgNPs act as remarkable antimicrobial agent against several Gram- Positive and Negative HPB strains. Maximal growth inhibition zone in *Salmonella typhimurium* (NCIM 2501) and a minimal inhibition zone in *Bacillus subtilis* (NCIM 2920) were observed at concentration of 80μg mL^{-1}. High activity of photocatalytic degradation of methylene blue (MB) at about 94.67% was observed under UV-light irradiation when the reaction time was extended 30 min. The multi-functionality of EWE-AgNPs may be useful for many industrial applications such as catalysis to waste water treatment in near future. Copyright © VBRI Press.

Keywords: Multi-functional AgNPs, UV-light irradiation, human pathogenic bacteria, antibacterial efficacy, photocatalytic degradation.

Introduction

Water availability has decreased recently due to its overuse, multiple contaminations, and due to erratic rainfalls in a scenario of climate change. Different sources of water pollutants increasingly deteriorate environmental water quality and health hazards [**1**]. Since many dyes are an important class of synthetic organic chemical compounds that are generally non-biodegradable such as methylene blue (MB), acid red 14, remazol red (RR), reactive blue 19, and methyl orange (MO) and providing major ecological problems [**2**]. At the same times, contaminated water sources caused by pathogenic microbes is considered to be a public health issue; which further results in the outbreak of waterborne hepatitis disease. The World Health Organization (WHO) has estimated special concern towards a rising emergency of antibiotic resistance of various human pathogens, not only for curing infectious diseases, but for other pathogens as well wherever antibiotic prophylaxis is required in order to avoid associated infections [**3**]. Presently, discharge of higher concentration of antibiotics to aquatic systems is major issue in geological terms.

Several studies have described the controlled synthesis of biocompatible nanoparticles of different sizes and shapes mediated by biomolecules, which is non-toxic, low-cost and minimizes environmental health hazards and environment damage [**4, 5**]. Recent literature reports encouraging results about the bactericidal activity and photocatalysis using semiconductor of silver nanoparticles (AgNPs) of either a simple or composite nature to remediate organic pollutants in the aqueous environment.

Experimental methods

Synthesis and characterization of biocompatible AgNPs

Silver nitrate ($AgNO_3$, analytical grade-Merck, India) and fresh eggs was purchased from a local supermarket. 5 mL of fresh egg white extract (EWE) was dissolved in 95 mL of distilled water with a strong magnetic stirrer for 30 min, and then the cloudy white solution was filtered by using a Whatman No.1 filter a clear solution was obtained and stored in a refrigerator at 4 ^{0}C until further processing. 90 mL of EWE to 10 mL of 1 mM $AgNO_3$ solution was added rapidly under vigorous stirring for 15 min and incubated in a boiling water bath at 70 ^{0}C for 30 min and it was observed that the solution gradually changed from white color to yellow color [**6**]. The remarkable color changed EWE-AgNPs confirmed by UV-Vis spectroscopy, FT-IR spectroscopy, X-ray diffraction (XRD) pattern and scanning electron microscopy (SEM) equipped with energy dispersive spectroscopy (EDS) have been used in the characterization.

Human pathogenic bacteria (HPB) for in-vitro antimicrobial screening

Test organisms HPB were obtained from the Council of Scientific and Industrial Research - National Chemical Industrial Microorganisms (CSIR-NCIM) as per our earlier report [**7**]. Biosynthesized EWE-AgNPs

powder was dissolved in Milli-Q water and sonicated for 20 min in order to prevent the particles agglomeration. Agar well diffusion assay was used to evaluate an *in-vitro* antibacterial activity of EWE and green EWE-AgNPs against certain bacterial strains on MHA plates [**8**]. Four wells each of 6 mm diameters were made on lawns of bacterial strains that coated each MHA plate. Then, EWE and dissolved EWE-AgNPs solutions were loaded into each well at different concentrations such as 20, 40, 60, and 80 µg mL^{-1}, respectively. The plates were incubated at 37 ± 2 ^{0}C for 24 - 48 hrs, the size of the diameter in the inhibition zone [**9, 10**].

EWE-AgNPs catalytic decolorization of methylene blue (MB) dyes

Photocatalytic activities of EWE-AgNPs were evaluated for the detoxification of methylene blue (MB) dye in an aqueous solution under UV-light irradiation. Suspensions were prepared by dissolving 75 mg of EWE-AgNPs in 200 mL of 10^{-5}M MB dye aqueous stock solution and these were maintained throughout reaction by circulating cold water at room temperature. Before illumination, the suspension was constantly magnet-stirred in an immersion well reactor for 30 min at dark condition in order to ensure a constant adsorption/ desorption equilibrium between EWE-AgNPs catalyst and dye molecules. After 30 min, 2 mL of the dispersed solution was taken at regular time intervals and centrifuged to remove the catalyst and the results confirmed by determining the MB dye concentration using UV-Vis spectroscopy [**11**]. From the resulting relation the percentage of degradation efficiency was calculated as follows:

$$\text{Degradation efficiency } \% = (c_o - c_t / c_o) \times 100 \quad (1)$$

where c_o represented the concentration of dyes before degradation and c_t represented the concentration of dyes after degradation [**12**].

Statistical analysis (ANOVA)

One-way analysis of variance was used to find whether there are any statistically significant differences between the variables and also understand their relationship by using the statistical package ORIGIN8.0.

Results and discussion

Structural, optical, and morphological properties of EWE-AgNPs

In the present decade urgent need to develop non-toxic or eco-friendly semiconductors based AgNPs. Fresh egg white extract (EWE) produced a remarkable color change from white to yellow color during the reaction, which confirmed the generation of EWE-AgNPs where Ag^+ ions are reduced to Ag^0 ions by the addition of 1 mM $AgNO_3$ which was substantiated through visual assessments. Further, carboxyl, hydroxyl, and amine functional groups in the biomolecules own the capability to decrease the metal ion and cap the newly formed EWE-AgNPs. The formation of EWE-AgNPs was confirmed by using UV-visible a maximum absorption of 422 nm recorded (**Fig. 1a**). FTIR bands were found at 3403 cm^{-1}, 2185 cm^{-1}, 1732 cm^{-1} and 1301 cm^{-1} (**Fig. 1b**). Absorption peak confirmed the presence of phenolic compounds with a O–H stretching (hydroxyl group) of polymeric association, amide II (N=H) bonds of proteins, amide I-group might have been formed owing to carbonyl stretching of proteins and a small peak detected the coupling interaction stretching of C-N, i.e., a deformation of N-H as well as C-H stretching, respectively. Thus, phenolic compounds having 1 or more aromatic rings and proteins/peptides play a important role in EWE-AgNPs formation. The XRD pattern four strong peaks were observed at 32.5^0, 46.4^0, 57.4^0 and 76.3^0. They were indexed to the 111, 200, 220, and 311 lattice planes of Ag^+, respectively (**Fig. 1c**). It was indicated that the particles had acceptable crystalinity with the face centered cubic (fcc) structure in the form of AgNPs aggregates. Average crystallite size of the nanoparticles was determined through Scherer's formula:

$$D = (k \lambda / \beta \cos \theta) \times 100 \quad (2)$$

where, K is the shape factor (k = 0.9); β is the full width at half maximum (FWHM); θ is the Bragg's angle; λ is the x-ray wavelength (λ = 1.5406) and found to be 21 nm.

The size, shape and morphological structure of EWE-AgNPs were documented through SEM analysis. The images showed a spherical particle size ranging from 15-60 nm (**Fig. 1d**). Energy dispersive spectroscopy (EDS) analysis implied a reduction of the silver ions to elemental Ag^+ signals that peaked at higher percentages of 95.77 (AgNPs) and other carbon elements comprised a portion of 4.23 percent and displayed a dominant peak at 3 KeV as a result.

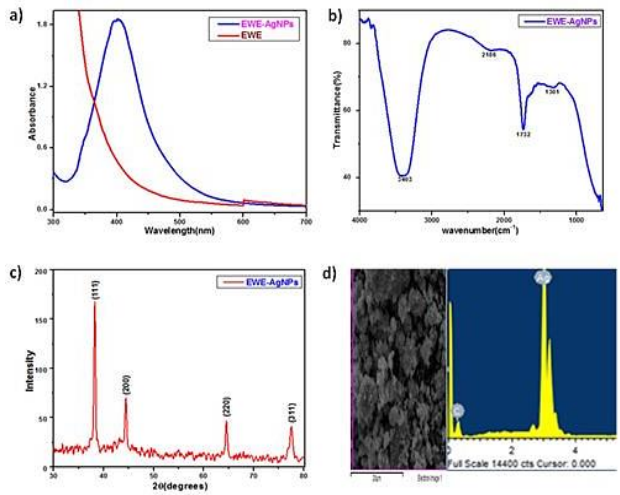

Fig. 1. (a) UV-Vis spectra spectrum (b) FTIR spectra (c) XRD pattern mixed phase (d) SEM and EDS image of synthesized EWE-AgNPs.

In-vitro antimicrobial screening study

Fig. 3 clearly illustrate the antimicrobial activity of biocompatible EWE-AgNPs. It is seen that, Gram-Negative HPB strains have noticeable activities *Salmonella typhimurium* (B5-NCIM 2501) maximal growth inhibition zone of 18 mm and a minimal inhibition zone were observed in Gram- Positive *Bacillus subtilis* (B1-NCIM 2920) in 10 mm at concentration of 80 µg mL^{-1}. The results of antimicrobial efficacy of different concentrated EWE-AgNPs were compared with each other and exhibited significant difference in the results ($p < 0.001$) (**Table 1**). The antimicrobial activities are varied depending upon the Gram-Positive and Negative HPB strains due to the extracellular polymeric substance (EPS) secretion [**13**]. Binding of many antibiotics to their specific targets (higher affinity) averts the normal activity of the target. In fact, bactericidal activity relies on the shape, size, and biosynthesized nanostructures (AgNPs) dosage, which were seen to bind the thiol groups of bacterial proteins, DNA and RNA affect.

Table 1. One-way analysis of variance (ANOVA) for different variables such as antimicrobial activity of EWE-AgNPs with different concentrations.

Concentrations of EWE-AgNPs	DF	Sum of Squares	Mean Square	F Value	Prob>F*
20µg mL^{-1}					
Model	4	1.76E+02	4.39E+01	109.75	3.23E-08
Error	10	4.00E+00	4.00E-01		
Total	14	1.80E+02			
40µg mL^{-1}					
Model	4	4.43E+01	1.11E+01	15.09091	3.07E-04
Error	10	7.33E+00	7.33E-01		
Total	14	5.16E+01			
60µg mL^{-1}					
Model	4	9.29E+01	2.32E+01	12.90741	5.84E-04
Error	10	1.80E+01	1.80E+00		
Total	14	1.11E+02			
80µg mL^{-1}					
Model	4	1.12E+02	2.81E+01	13.17187	5.37E-04
Error	10	2.13E+01	2.13E+00		
Total	14	1.34E+02			

* $p < 0.001$ – The variable means are significantly different

Photocatalytic degradation of MB dye

Photocatalytic activities of EWE-AgNPs were evaluated *via* photodegradation of MB dye under UV-light irradiation results are shown in **Fig. 2b, c** and **d**. A blank test was conducted without add EWE-AgNPs for MB dye results in minimal degradation (8.26%) shows no color change. Subsequently degradation was carried out in the presence of EWE-AgNPs catalyst accounting for 94.67%, when exposed to UV-light irradiation. The dye degradation rate was highly depended on the morphology and crystallinity of biosynthesized EWE-AgNPs. The notable photocatalytic performance was majorly owing to the occurrence of surface proteins that act as a competent host for MB and also aids the absorption of MB dye with low recombination rate of e^-/h^+ pairs. The ecofriendly, cost-effectiveness features of the present method for ‘‘one-pot’’ synthesis and AgNPs modification can be used to synthesize other NPs and further, it could be used in various avenues of research field.

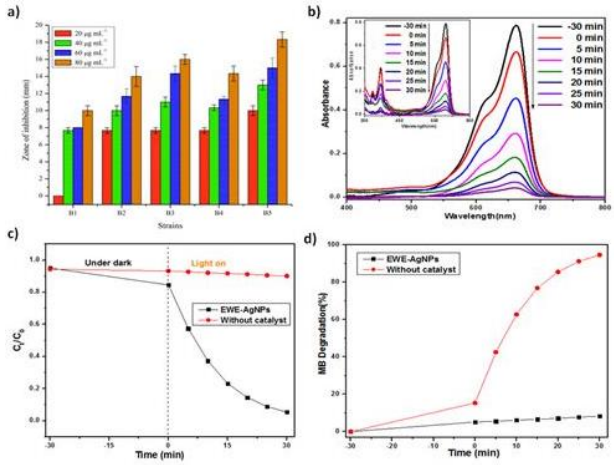

Fig. 2. (a) *In-vitro* antibacterial activity; (b), (c) and (d) Photodegradation of methylene blue (MB) dyes with EWE-AgNPs under UV-light irradiation.

Conclusions

This study proved that EWE-AgNPs were effective against different HPB isolates and it showed maximum inhibition of *S. typhimurium* (18 mm) and minimum inhibition of *B. subtilis* (10 mm). EWE -AgNPs are likely to rupture the membrane of bacterial cell walls and EPS secretion *via* binding with intracellular materials were likely responsible for the onset of rapid cell death. EWE-AgNPs exhibited superior degradation activity of MB dye up to 94.67% compared to without add catalyst under UV-light irradiation 8.26% were recorded at 30 min. The combined effect (UV-light condition + EWE-NPs) encourages the development of eco-friendly, less cost and easy synthesized antimicrobial agents and highly efficient photocatalyst to eliminate dye pollutants.

Acknowledgments

The author K. Muthukumar wishes to thank the Department of Science and Technology, Science Engineering Research Board (DST-SERB), New Delhi, India for the award of a National Postdoctoral fellowship (PDF/2017/002213) to undertake a part of this study.

References

1. Sacco, O.; Stoller, M.; Vaiano, V.; Ciambelli, P.; Chianese, A.; Sannino, D.; *Int. J. Photoenergy*, **2012**, 1.
2. Gai, L.; Duan, X.; Jiang, H.; Mei, Q.; Zhou, G.; Tian, Y.; *Cryst. Eng. Comm.*, **2012**, *14*, 7662.
3. Matos, R.A.; Courrol, L.C.; *Colloids and Surfaces A: Physicochem. Eng. Aspects*, **2014**, *441*, 539.
4. Humphrey, S.P.; Williamson, R.T.; *J. Prosth. Dent.*, **2001**, 85, 162.

5. Lu, R.; Yang, D.; Cui, D.; Wang, Z.; Guo, L.; Inter. *J. Nanomed.*, **2012**, *7*, 2101.
6. Krishnan, M.; Subramanian, H.; Hans-Uwe, D.; Sivanandham, V.; Seeni, P.; Gopalan, S.; Mahalingam, A.; Rathinam, A.J.; *Sci. Rep.*, **2018**, *8*, 2609.
7. Krishnan, M.; Hans-Uwe, D.; Seeni, P.; Gopalan, S.; Sivanandham, V.; Jin-Hyoung, K..; James, R.A.; *Mater. Sci. Eng. C.*, **2017**, *73*, 743.
8. Vignesh, S.; Karthikeyan, B.; Udayabhaskar, R.; Arjunan, V.; Ashok, M.; Narayana Kalkura, S.; James. R.A.; Asian. *J. Physics.*, **2014**, *23*, 1025.
9. Vignesh, S.; Muthukumar, K.; James, R.A.; *Mar. Poll. Bull.*, **2012**, *64*, 790.
10. Zhao, J.; Zhao, Z.; Li, N.; Nan, J.; Yu, R.; Du, J.; *Chem. Eng. J.*, **2018**, *353*, 805.
11. Goutam, S.P.; Saxena, G.; Singh, V.; Yadava, A.K.; Bharagava, R.N.; Thapa, K.B.; *Chem. Eng. J.*, **2018**, *336*, 386.
12. Marambio-Jones, C.; Hoek, E.M.V.; *J. Nanopart. Res.*, **2010**, *12*, 1531.
13. Krishnan, M.; Sivanandham, V.; Hans-Uwe, D.; Murugaiah, S.G.; Seeni, P.; Gopalan, S.; Rathinam, A.J.; *Mar. Poll. Bull.*, **2015**, *101*, 816.

